Available online at www.sciencedirect.com

ScienceDirect

IFAC PapersOnline CONFERENCE PAPER ARCHIVE

IFAC-PapersOnLine 48-12 (2015) 340–345

Stability Analysis of Machining Processes Using Spectral Element Approach

Firas A. Khasawneh *

* *SUNY Polytechnic Institute, Mechanical Engineering, Utica, NY 13502, USA(e-mail: firas.khasawneh@sunyit.edu)*

Abstract: The stability analysis of machining processes is of utmost importance in order to guarantee high removal rates while at the same time maintaining acceptable surface finish and tool life. One of the key mechanisms for losing stability in machining is chatter vibration, which is a self-excited vibration due to the surface regeneration effect. This type of chatter occurs due to the variation in the dynamic cutting load between successive tool or workpiece rotations. A common approach to capture this dependency on prior states is to model the machining process using delay differential equations. Since chatter has detrimental effects on the cutting process, the ability to predict the combinations of the cutting process parameters that will result in chatter-free cutting is highly desirable. In this paper we describe how the stability of turning and milling processes can be studied using the spectral element approach. The results show that this approach can successfully predict the chatter-free regime in turning and milling. Further, we describe how recent numerical implementations of the approach to a wider class of delay equations can enable the analysis of more complex and realistic machining models.

Keywords: Machining, Spectral analysis, Stability, Time delay, Time domain analysis

1. INTRODUCTION

Conventional material removal processes such as turning and milling still constitute a large class of modern machining processes. Therefore, it is beneficial to optimize these processes such that the maximum amount of material is removed while at the same time satisfying important manufacturing constrains such as the surface quality, tool life, and noise level.

One of the most prominent problems in machining processes is regenerative chatter which is typically referred to simply as chatter (Quintana and Ciurana (2011)). These variations are the result of the phase shift between the cutting marks left on the surface between successive tool/workpiece revolutions. A well-accepted mechanism for explaining and describing chatter includes delays in the governing equation of the system. The resulting delay differential equations (DDEs), which also appear in many areas of science and engineering, have been an active topic of research for over six decades. Both frequency (Altintaş and Budak (1995); Otto et al. (2014)) and time domain (Insperger and Stépán (2004); Butcher et al. (2009); Khasawneh et al. (2012)) methods were developed to ascertain the stability of machining models. One of the recent methods that has been successfully used to study the stability of delay differential equations is the spectral element method (Khasawneh and Mann (2011a)). The spectral element approach is robust and flexible and it is capable of fast convergence as was shown in Tweten et al. (2012). Therefore, it can have useful applications in the study of machining models and delay equations in general.

In this paper the stability analysis of DDEs using the spectral element approach (SEA) is first described. We then use the SEA to study the stability of a turning and a milling model. The resulting stability diagrams, which chart the chatter and the chatter-free regime in the space of the cutting depth and the spindle speed, are presented and compared to results from the literature. The paper concludes with some available and some possible extensions for the approach.

2. STABILITY ANALYSIS WITH SPECTRAL ELEMENT METHOD

In order to simplify the presentation, we describe the stability analysis for systems of the form

$$\frac{dx}{dt} = A(t)x(t) + B(t)x(t-\tau), \tag{1}$$

where A and B are the $d \times d$ system matrices, and τ is the time delay. In this paper, we consider the autonomous $(A(t) = A, B(t) = B)$ case and the non-autonomous time-periodic case $(A(t+T) = A(t), B(t+T) = B(t))$, and we study the corresponding stability of stationary solutions (autonomous case) and periodic orbits (non-autonomous case) of (1). Although the approach can be used for arbitrary T to τ ratios (Khasawneh and Mann (2013)), we restrict the presentation to the case $\tau = T$, i.e., to constrained meshes.

Since it is often impossible to deal directly with the infinite dimensional DDE (1), it must first be discretized to produce a finite dimensional approximation. The idea is that as the degree of approximation increases, the solution of the finite dimensional problem converges to that of the infinite dimensional problem. The goal of the approximation is to construct a finite dimensional dynamic map in the form

$$x_m = U x_{m-1}, \tag{2}$$

2405-8963 © 2015, IFAC (International Federation of Automatic Control) Hosting by Elsevier Ltd. All rights reserved.
Peer review under responsibility of International Federation of Automatic Control.
10.1016/j.ifacol.2015.09.401

where x_m and x_{m-1} are the vectors of the discretized states on $[-\tau + T, T]$ and $[-\tau, 0]$, respectively, whereas U is the monodromy matrix, which represents a finite dimensional approximation to the infinite dimensional monodromy operator. The monodromy operator U corresponds to the evolution family E of the linearized system (Diekmann et al. (1995)) evaluated in the coefficients' period T with initial instant 0, i.e., $U = E(T, 0)$. This operator maps the initial state defined on $[-\tau, 0]$ into the state one T later, $[T - \tau, T]$. The stability of the system is then investigated using the eigenvalues of U according to the criteria shown in Fig. 1.

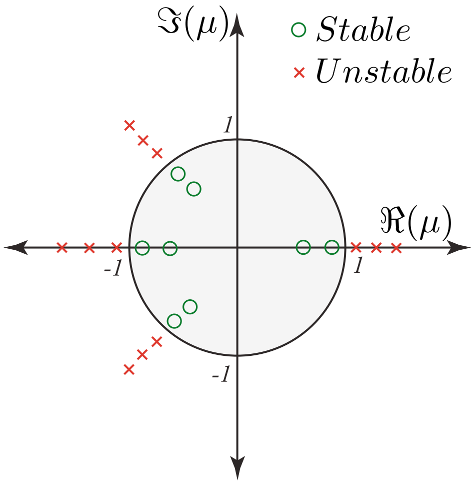

Fig. 1. The stability criteria dictates that all the eigenvalues, μ, of the monodromy operator U, should lie within the unit circle in the complex plane.

The first step for ascertaining the stability of (1) using SEA is to discretize the period $[0, T]$ using a finite number of temporal elements E. Each element is described by the interval

$$e_j = [t_j^{\mathrm{L}}, t_j^{\mathrm{R}}), \tag{3}$$

where t_j^{L} and t_j^{R} denote the left and right element boundaries, respectively, with the length of the jth element given by

$$h_j = t_j^{\mathrm{R}} - t_j^{\mathrm{L}}. \tag{4}$$

The index j starts at the leftmost element on the time line, i.e., $e_1 = [-\tau, -\tau + h_1)$. A local normalized time $\eta = \sigma/h_j$ is defined within each element where $\sigma \in [0, h_j]$ is the local time while $\eta \in [0, 1]$. The barycentric Lagrange formula is then used to obtain an approximate expression for the states over each element using $n+1$ distinct, local interpolation nodes normalized by h_j according to

$$x_j(t) = \sum_{i=1}^{n+1} \phi_i(\eta) x_{ji}, \tag{5}$$

where $x_{ji} = x_j(t_i)$ with i indicating the ith local interpolation node, and ϕ_i are the trial functions that can be calculated using the barycentric Lagrange formula in Higham (2004)

$$\phi_i(\eta) = \frac{\frac{\varpi_i}{\eta - \eta_i}}{\sum_{k=1}^{n+1} \frac{\varpi_k}{\eta - \eta_k}}, \tag{6}$$

where for node η_k the trial functions must satisfy

$$\phi_i(\eta_k) = \begin{cases} 1, & i = k \\ 0, & i \neq k. \end{cases} \tag{7}$$

while the barycentric weights ϖ_k are given by

$$\varpi_k = \frac{1}{\prod_{k \neq j} (\eta_j - \eta_k)}, \qquad j = 1, \ldots, n+1. \tag{8}$$

In this study we use (6) to obtain the trial functions since it has better numerical stability and requires less computation than the conventional Lagrange representation, see Berrut and Trefethen (2004); Higham (2004). The barycentric weights can also be used to obtain the value of the derivative of the trial functions evaluated at the interpolation nodes according to

$$\phi_i'(\eta_k) = \begin{cases} \dfrac{\varpi_i/\varpi_k}{\eta_i - \eta_k}, & i \neq k \\ \displaystyle\sum_{i=0, i\neq k}^{n+1} \dfrac{-\varpi_i/\varpi_k}{\eta_i - \eta_k}, & i = k \end{cases}. \tag{9}$$

Substituting the expression from (5) into (1) gives

$$\sum_{i=1}^{n+1} \frac{1}{h_j} \dot{\phi}_i(\eta) x_{ji} - A(t_j^{\mathrm{L}} + \eta) \sum_{i=1}^{n+1} \phi_i(\eta) x_{ji} - B(t_j^{\mathrm{L}} + \eta) \sum_{i=1}^{n+1} \phi_i(\eta) x_{(j-n_e),i} = \text{error}, \tag{10}$$

where the residual error is due to the approximation procedure while n_e indicates the number of elements used to discretize the states in $[0, T]$. We emphasize that this presentation assumes a constrained mesh and temporal elements of uniform length.

We minimize the errors in a weighted integral sense (10) (Reddy (1993)) over each temporal element. Specifically, (10) is multiplied by a set of independent weight functions $\psi_p(\eta)$ where $p = 1, 2, \ldots, n$ and is integrated over the normalized length of each element within the constrained mesh according to

$$\int_0^1 \left[\sum_{i=1}^{n+1} \frac{1}{h_j} \dot{\phi}_i(\eta) x_{ji} - A(t_j^{\mathrm{L}} + \eta) \sum_{i=1}^{n+1} \phi_i(\eta) x_{ji} - B(t_j^{\mathrm{L}} + \eta) \sum_{i=1}^{n+1} \phi_i(\eta) x_{j^*,i} \right] \psi_p(\eta)\, d\eta = 0. \tag{11}$$

In this study we chose the weight functions to be the set of the n shifted Legendre polynomials.

The weighted residual integral in Eq. (11) is often difficult to evaluate analytically. Therefore, analytical integration is substituted by a quadrature rule which uses $n+1$ quadrature points over each element, which coincide with the $n+1$ interpolation nodes, according to

$$\sum_{k=1}^{n+1} w_k \left(\sum_{i=1}^{n+1} \frac{1}{h_j} \dot{\phi}_i(\eta_k) x_{ji} - A(t_j^{\mathrm{L}} + \eta_k) \sum_{i=1}^{n+1} \phi_i(\eta_k) x_{ji} - B(t_j^{\mathrm{L}} + \eta_k) \sum_{i=1}^{n+1} \phi_i(\eta_k) x_{j^*,i} \right) \psi_p(\eta_k) = 0, \tag{12}$$

where η_k and w_k are the quadrature nodes and weights, respectively.

To construct a dynamic map, each discretization point in $[0, T]$ is mapped by τ. Since (1) is linear in x_{ji} and

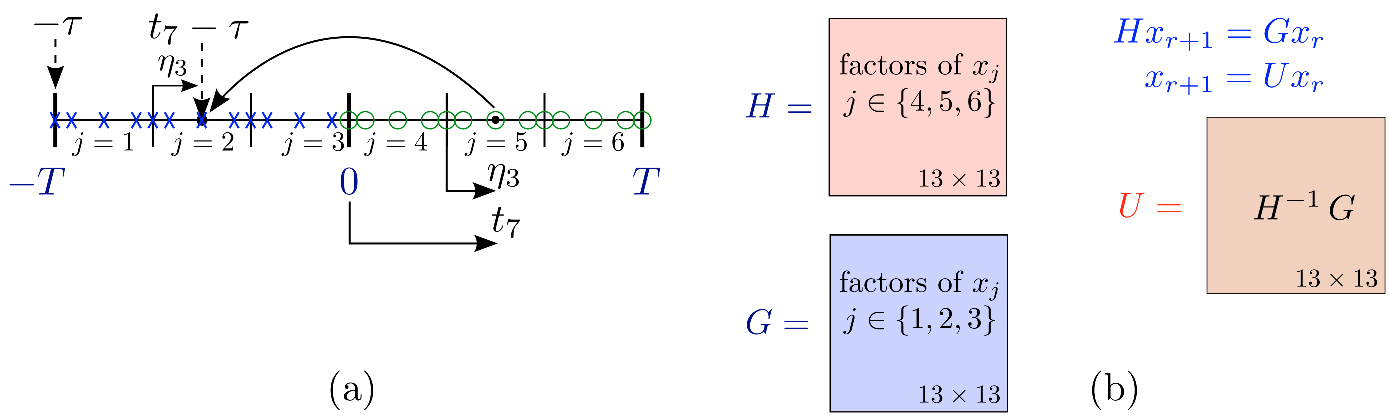

Fig. 2. Example discretization of the state-space over the period T when $\tau = T$. Figure (a) shows the discretization of the time-line over each T using 3 temporal elements with 5 nodes within each element. Figure (b) describes the sizes of the resulting map matrices H, G, and U when the DDE is assumed to be of first order.

$x_{j^*,i}$, applying (12) to all the elements using the n weight functions yields a set of $d \times n$ algebraic equations (d is the order of the DDE). In addition, enforcing a condition that relates the discretized states from the previous period to the states at $t = 0$ gives d additional equations for a total of $d(n + 1)$ equations. We note here that the conditions providing the continuity at the end points of neighboring elements (that is $x_{j-1,n+1} = x_{j,1}$) are embedded into the vectors x_m and x_{m-1}.

Consider for example the state-space discretization shown in Fig. 2a for a DDE with $\tau = T$. The goal here is to approximate the monodromy matrix by constructing a map between the delayed states denoted by the blue 'X' and the states one period ahead, denoted by the green 'O'. Notice that the interval $[0, T]$ was discretized using 3 elements and 5 interpolation nodes within each element. To describe mapping the states, consider the 3rd node within the 5th element. The local time for this node is η_3 while the global time is t_7 since globally this is the 7th node. Since $T = \tau$, due to the delay τ this node will look back at a corresponding node in the previous period and the local time for that delayed node will also be η_3. Therefore, for the case $T = \tau$ no interpolation is necessary since the delayed states always line up with a mesh point. Mapping all the discretized states in $[0, T]$ is done in a similar fashion. All the coefficients multiplying the states on $[0, T]$ are arranged into a matrix H whereas the coefficients multiplying the states on $[-T, 0]$ are arranged into another matrix G.

Using the example discretization in Fig. (2)a and assuming the DDE is of first order, then the sizes of the resulting H and G matrices are shown in Fig. 2b. Recall that the stability is determined by the eigenvalues of the monodromy matrix $U = H^{-1}G$. Note that for this case the entries are block matrices aligned in a band near the diagonal and all the entries off this band are zeros except the last d rows. These last d rows in both the H and the G matrix contain the $d \times d$ identity matrix multiplying the point $x(0)$ to enforce the continuity condition at $t = 0$.

The coefficients of the discretized states in the intervals $[0, T]$ and $[-T, 0]$ can be arranged into two matrices: H and G, respectively. The resulting mapping from the states $x_m \in [0, T]$ onto $x_{m-1} \in [-T, 0]$ is described by the dynamic map

$$x_m = H^{-1}Gx_{m-1} = Ux_{m-1}. \tag{13}$$

where $U = H^{-1}G$ is the monodromy matrix described in (2). Alternatively, the inversion of H can be avoided by solving the generalized eigenvalue problem $|G - \mu H| = 0$ for the eigenvalues μ. The stability of (1) is then ascertained by examining the eigenvalues μ (or characteristic multipliers) of U: the system is stable if all the eigenvalues are within the unit circle in the complex plane, as shown in Fig. 1.

The case of autonomous DDEs or of DDEs with $T = \tau$ results in a constrained mesh where each temporal element in $[-\tau, 0]$ is mapped exactly onto a corresponding element in $[-\tau + T, T]$. When these cases are combined with an appropriate choice of discretization points, such as Legendre-Gauss points, the SEA gives rise to fast convergence as the number of points is increased (called super-convergence, see Engelborghs et al. (2000)).

3. STABILITY ANALYSIS OF A TURNING MODEL

As a first example to demonstrate the applicability of SEA to machining models, we investigate the stability in turning a rigid workpiece with a flexible too. We assume that the cutting tool is flexible along the y direction as shown in Fig. 4. The equation of motion for this single degree of freedom system can therefore be written as

$$\ddot{y} + 2\zeta\omega\dot{y} + \omega^2 y = \frac{F}{m}, \tag{14}$$

where ζ is the damping ratio, ω is the natural frequency of the tool, m is the modal mass, and F is the cutting force. We use the power model for the cutting force which is assumed to depend on the uncut chip thickness according to

$$F = K_y w h^{\alpha}, \tag{15}$$

where K_y is the mechanistic cutting coefficient, w is the depth of cut, h is the chip thickness, and the exponent is typically chosen as $\alpha = 0.75$. Due to the compliance of the tool, the chip thickness varies dynamically in time according to

$$h = \begin{cases} h_0 + y(t-\tau) - y(t) & \text{if } \; y(t) - y(t-\tau) \le h_0 \\ 0 & \text{otherwise} \end{cases} \tag{16}$$

where h_0 is the nominal feed rate per revolution while τ is the duration of one spindle rotation. To reduce the number of parameters in (14), we use the rescaling used in Insperger et al. (2008). Let $y(t) = h_0\tilde{y}(t)$ and rescale time such that $\tilde{t} = \omega t$ and $\tilde{\tau} = \omega\tau$. After dropping the tildes, the resulting equation reads

$$\begin{aligned}\ddot{y} + 2\zeta\dot{y} + y &= \frac{K_y w(2\pi R)^{\alpha-1}}{m\omega^2}\rho^{\alpha-1}(1 + y(t-\tau) - y(t))^\alpha \\ &= K\rho^{\alpha-1}(1 + y(t-\tau) - y(t))^\alpha \qquad (17)\end{aligned}$$

where R is the radius of the workpiece, $\rho = h_0/(2\pi R)$, and K is the dimensionless depth of cut. Typical values for ρ in conventional turning are $\rho < 0.01$. In this paper we assume that the tool remains in contact with the workpiece, i.e., we ignore the fly-over effect. From (17) it can be seen that the constant steady state solution is $K\rho^{\alpha-1}$.

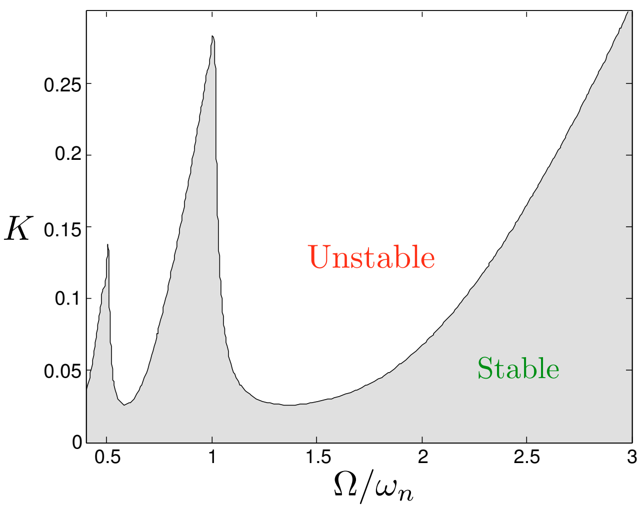

Fig. 3. The stability diagram for Eq. (18) using $\zeta = 0.03$, $\rho = 0.01$, and $\alpha = 0.75$.

Linearizing Eq. (17) around the steady state solution ,we get the linear delay differential equation

$$\ddot{\xi} + 2\zeta\dot{\xi} + y = \alpha K\rho^{\alpha-1}(\xi(t-\tau) - \xi(t)) \qquad (18)$$

Equation (17) describes the oscillations of the tool assuming a deterministic model and it will be used for obtaining the stability of the linearized deterministic system.

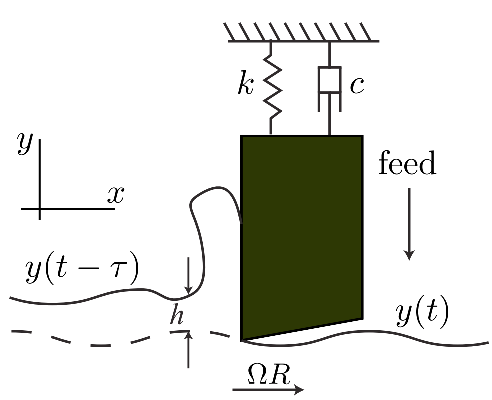

Fig. 4. The turning process under study in this paper. The tool is compliant in x while the workpiece is assumed rigid.

Equation (18) is linear autonomous delay differential equation whose stability can be studied using several methods in the literature, e.g., zero-order approximation (Altintaş and Budak (1995)), semi-discretization (Insperger and Stépán (2004)), Chebyshev collocation (Butcher and Bobrenkov (2011)), or spectral element method (Khasawneh and Mann (2011a)). In this study we use the spectral element method with one temporal element, a polynomial of degree 12, and a 100×100 grid in the $(\Omega/\omega_n, K)$ plane.

The resulting stability diagram is shown in Fig. 3 in the $(\Omega/\omega_n, b)$ space where Ω is the spindle speed in radians/seconds while ω_n is the natural frequency of the tool. Shaded regions are stable while unshaded regions are unstable. The results are in agreement with the analytical stability results for simple turning processes in Stépán (1989).

4. STABILITY ANALYSIS OF A MILLING MODEL

The SEA can also be used with non-autonomous machining models. For example, consider the schematic in Fig. 5 of a flexible milling tool (the workpiece is assumed to be rigid). The equation of motion for this system generalized for N straight cutting teeth is

$$\mathbf{M}\ddot{\mathbf{X}}(t)+\mathbf{C}\dot{\mathbf{X}}(t)+\mathbf{K}\mathbf{X}(t) = b\mathbf{K}_c(t)\left[\mathbf{X}(t) - \mathbf{X}(t-\tau)\right]+b\mathbf{f}_o(t) \qquad (19)$$

where $\mathbf{X}(t) = [x(t)\ \ y(t)]^T$ is the position vector of the tool tip, $\mathbf{M}$, $\mathbf{C}$ and $\mathbf{K}$ are the 2×2 mass, damping and stiffness matrices, while $\mathbf{K}_c$ and $\mathbf{f}_o$ are the τ-periodic specific cutting force variation matrix and stationary cutting force vector, respectively, where the tooth passage period in seconds is $\tau = 60/N\Omega$. The variables $\mathbf{K}_c(t)$ and $\mathbf{f}_0(t)$ are given by

$$\mathbf{K}_c(t) = \sum_{p=1}^{N} g_p(t)\begin{bmatrix} -K_t cs - K_n s^2 & -K_t c^2 - K_n sc \\ K_t s^2 - K_n cs & K_t sc - K_n c^2 \end{bmatrix}, \qquad (20a)$$

$$\mathbf{f}_o(t) = \sum_{p=1}^{N} g_p(t) f \begin{bmatrix} -K_t cs - K_n s^2 \\ K_t s^2 - K_n cs \end{bmatrix}, \qquad (20b)$$

where $s = \sin\theta_p(t)$, $c = \cos\theta_p(t)$, K_t and K_n are the tangential and normal cutting force coefficients, respectively, b is the nominal depth of cut, f is the nominal feedrate, and $g_p(t)$ is a switching function which is equal to one if the p^{th} tooth is active and zero if it is not cutting (Minis and Yanushevsky (1993); Tlusty (2000); Altintaş (2000); Davies and Balachandran (2000); Davies et al. (2002); Altintas et al. (2008)). The angle $\theta_p(t)$ is the angular position of the p^{th} tooth. For a cutter with evenly spaced teeth, $\theta_p(t) = (2\pi\Omega/60)t + p2\pi/N$ where Ω is the spindle speed given in revolutions per minute (or rpm) and N is the total number of cutting teeth.

When the structure is compliant only in a single direction, (19) is modified by eliminating the rows and columns corresponding to the non-compliant direction. For simplicity, we assume that the tool is only compliant in y and we write the simplified version of (19) in state space form according to

$$\dot{\mathbf{y}}(t) = \mathbf{A}\mathbf{y}(t) + \mathbf{B}\mathbf{y}(t-\tau) + \mathbf{c}. \qquad (21)$$

Equation (21) is now in the form described in (1), so the SEA can be used to study its stability. Since the term $\mathbf{c}$

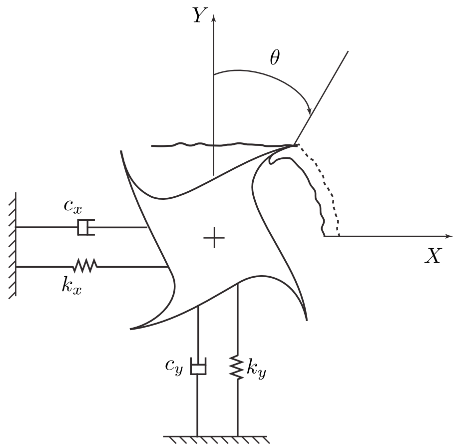

Fig. 5. Mechanical model of a 2 DOF milling operation.

does not affect the stability of the system, we omit it from the stability calculations.

Figures 6 and 7 show the stability diagrams for up- and down-milling, respectively, with 4 teeth and different values of the radial immersion (a_e). The parameters that were used in the model are shown in table 1. The stability diagrams were obtained on a 200×200 grid using one spectral element and a 30th order interpolation polynomial. The stability diagrams obtained using SEA agree with the ones obtained using a Chebyshev-based approach (Bobrenkov et al. (2010)).

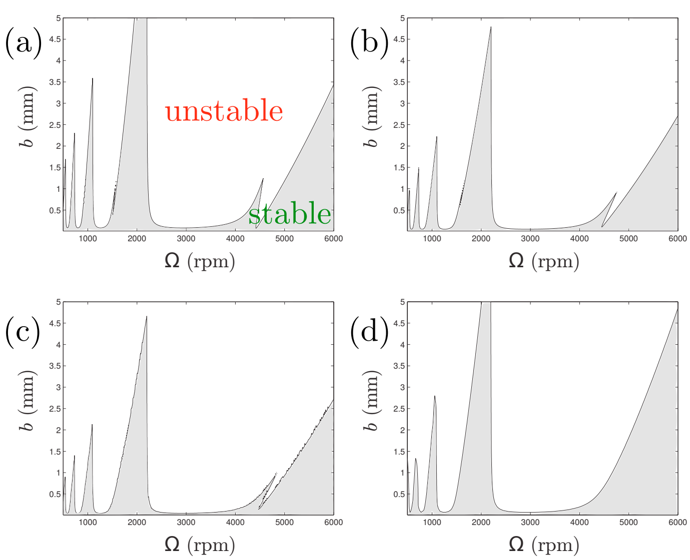

Fig. 6. Upmilling with 4-teeth and radial immersion (a_e) (a) $a_e = 0.25$, (b) $a_e = 0.5$, (c) $a_e = 0.75$, and (d) $a_e = 1.0$.

Process parameters	K_t (N/m^2)	K_n (N/m^2)	ζ
	5.5×10^8	2×10^8	0.0032
Tool parameters	m (kg)	ω_n (rad/s)	N
	2.5729	920.24	4

Table 1. The parameters used in the milling model.

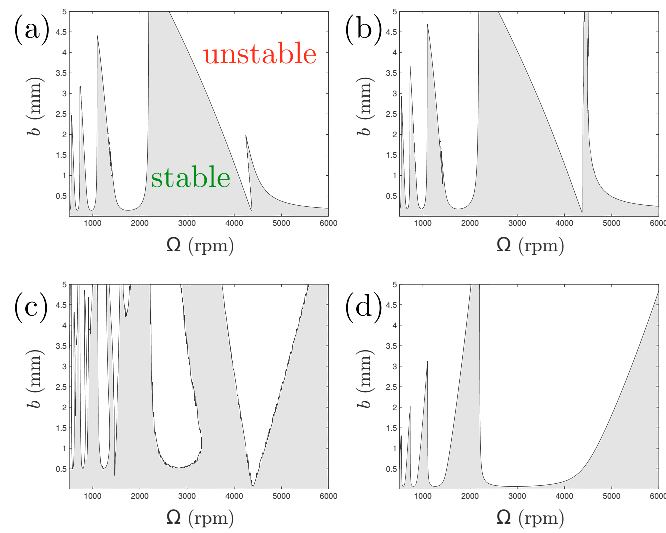

Fig. 7. Downmilling with 4-teeth and (a) $a_e = 0.25$, (b) $a_e = 0.5$, (c) $a_e = 0.75$, and (d) $a_e = 1.0$.

5. CONCLUSION

The spectral element approach allows refining both the order and the number of the spectral elements as well as their location which makes it a useful and flexible tool for studying the stability of machining processes. In addition to its flexibility, the SEA typically has high rates of convergence (Tweten et al. (2012)).

Although the SEA was presented here using two machining models with one discrete delay, it can also be used with more complicated models that include multiple discrete delays and distributed delays (Khasawneh and Mann (2011b, 2013)). These models emerge, for example, when milling with tools that have variable pitch or helical tools with variable helix angles.

Since the SEA is a time-domain approach, it is well-suited for non-autonomous systems. Future research directions include extending the approach to study the stability of linearized state-dependent delay models (Insperger et al. (2007)), machining of distributed components (Bravo et al. (2005)), and stochastic machining models (Buckwar et al. (2006); Kuske (2006); Otto et al. (2015)).

REFERENCES

Altintaş, Y. (2000). *Manufacturing Automation*. Cambridge University Press, New York, 1 edition. doi: 10.2277/0521659736.

Altintaş, Y. and Budak, E. (1995). Analytical prediction of stability lobes in milling. *CIRP Annals*, 44(1), 357–362.

Altintas, Y., Stepan, G., Merdol, D., and Dombovari, Z. (2008). Chatter stability of milling in frequency and discrete time domain. *{CIRP} Journal of Manufacturing Science and Technology*, 1(1), 35 – 44. doi: 10.1016/j.cirpj.2008.06.003.

Berrut, J. and Trefethen, L.N. (2004). Barycentric Lagrange interpolation. *SIAM Review*, 46(3), 501–517.

Bobrenkov, O., Khasawneh, F., Butcher, E., and Mann, B. (2010). Analysis of milling dynamics for simultaneously engaged cutting teeth. *Journal of Sound and Vibration*, 329(5), 585–606. doi:10.1016/j.jsv.2009.09.032.

Bravo, U., Altuzarra, O., de Lacalle, L.L., Sanchez, J., and Campa, F. (2005). Stability limits of milling considering the flexibility of the workpiece and the machine. *International Journal of Machine Tools and Manufacture*, 45(15), 1669 – 1680. doi: 10.1016/j.ijmachtools.2005.03.004.

Buckwar, E., Kuske, R., L'Esperance, B., and Soo, T. (2006). Noise-sensitivity in machine tool vibrations. *International Journal of Bifurcation and Chaos*, 16(08), 2407–2416. doi:10.1142/S021812740601615X.

Butcher, E., Bobrenkov, O., Bueler, E., and Nindujarla, P. (2009). Analysis of milling stability by the Chebyshev collocation method: Algorithm and optimal stable immersion levels. *Journal of Computational and Nonlinear Dynamics*, 4(3), 031003. doi:10.1115/1.3124088.

Butcher, E.A. and Bobrenkov, O.A. (2011). On the chebyshev spectral continuous time approximation for constant and periodic delay differential equations. *Communications in Nonlinear Science and Numerical Simulation*, 16(3), 1541 – 1554. doi: http://dx.doi.org/10.1016/j.cnsns.2010.05.037.

Davies, M.A., Pratt, J.R., Dutterer, B., and Burns, T.J. (2002). Stability prediction for low radial immersion milling. *Journal of Manufacturing Science and Engineering*, 124(2), 217–225. doi:10.1115/1.1455030.

Davies, M. and Balachandran, B. (2000). Impact dynamics in milling of thin-walled structures. *Nonlinear Dynamics*, 22(4), 375–392. doi:10.1023/A:1008364405411.

Diekmann, O., Gils, S., Lunel, S., and Walther, H.O. (1995). *Delay Equations: Functional-, Complex-, and Nonlinear Analysis*. Springer.

Engelborghs, K., Luzyanina, T., in 'T Hout, K.J., and Roose, D. (2000). Collocation methods for the computation of periodic solutions of delay differential equations. *SIAM J. Sci. Comput.*, 22, 1593–1609. doi: 10.1137/S1064827599363381.

Higham, N.J. (2004). The numerical stability of barycentric lagrange interpolation. *IMA Journal of Numerical Analysis*, 24(4), 547–556. doi: 10.1093/imanum/24.4.547.

Insperger, T. and Stépán, G. (2004). Updated semi-discretization method for periodic delay-differential equations with discrete delay. *International Journal for Numerical Methods*, 61, 117–141.

Insperger, T., Stépán, G., and Turi, J. (2007). State-dependent delay in regenerative turning processes. *Nonlinear Dynamics*, 47, 275–283. doi:10.1007/s11071-006-9068-2.

Insperger, T., Barton, D.A., and Stepan, G. (2008). Criticality of hopf bifurcation in state-dependent delay model of turning processes. *International Journal of Non-Linear Mechanics*, 43(2), 140 – 149. doi: http://dx.doi.org/10.1016/j.ijnonlinmec.2007.11.002.

Khasawneh, F.A., Bobrenkov, O.A., Mann, B.P., and Butcher, E.A. (2012). Investigation of period-doubling islands in milling with simultaneously engaged helical flutes. *Journal of Vibration and Acoustics*, 134(2), 021008. doi:10.1115/1.4005022.

Khasawneh, F.A. and Mann, B.P. (2011a). A spectral element approach for the stability of delay systems. *International Journal for Numerical Methods in Engineering*, 87(6), 566–592. doi:10.1002/nme.3122.

Khasawneh, F.A. and Mann, B.P. (2011b). Stability of delay integro-differential equations using a spectral element method. *Mathematical and Computer Modelling*, 54, 2493–2503. doi:10.1016/j.mcm.2011.06.009.

Khasawneh, F.A. and Mann, B.P. (2013). A spectral element approach for the stability analysis of time-periodic delay equations with multiple delays. *Communications in Nonlinear Science and Numerical Simulation*, 18(8), 2129 – 2141. doi: http://dx.doi.org/10.1016/j.cnsns.2012.11.030.

Kuske, R. (2006). Multiple-scales approximation of a coherence resonance route to chatter. *Computing in Science Engineering*, 8(3), 35–43. doi: 10.1109/MCSE.2006.44.

Mann, B.P. and Young, K.A. (2006). An empirical approach for delayed oscillator stability and parametric identification. *Proceedings of the Royal Society A*, 462, 2145–2160.

Minis, I. and Yanushevsky, R. (1993). A new theoretical approach for prediction of machine tool chatter in milling. *Journal of Engineering for Industry*, 115, 1–8.

Otto, A., Rauh, S., Kolouch, M., and Radons, G. (2014). Extension of tlusty's law for the identification of chatter stability lobes in multi-dimensional cutting processes. *Int. J. Mach. Tools Manuf.*, 82-83, 50 – 58.

Otto, A., Khasawneh, F., and Radons, G. (2015). Position-dependent stability analysis of turning with tool and workpiece compliance. *The International Journal of Advanced Manufacturing Technology*, 1–11. doi:10.1007/s00170-015-6929-1. URL `http://dx.doi.org/10.1007/s00170-015-6929-1`.

Quintana, G. and Ciurana, J. (2011). Chatter in machining processes: A review. *International Journal of Machine Tools and Manufacture*, 51(5), 363–376. doi: 10.1016/j.ijmachtools.2011.01.001.

Reddy, J. (1993). *An Introduction To The Finite Element Method*. McGraw-Hill, Inc., New York, NY, 2 edition.

Tlusty, J. (2000). *Manufacturing Processes and Equipment*. Prentice Hall, Upper Saddle River, NJ, 1 edition.

Tweten, D.J., Lipp, G.M., Khasawneh, F.A., and Mann, B.P. (2012). On the comparison of semi-analytical methods for the stability analysis of delay differential equations. *Journal of Sound and Vibration*, 331(17), 4057–4071. doi:10.1016/j.jsv.2012.04.009.

Stépán, G. (1989). *Retarded Dynamical Systems: Stability and Characteristic Functions*. John Wiley & Sons.